Astron. Astrophys. 355, 165–170 (2000)

ASTRONOMY AND ASTROPHYSICS

A search for extended disks around weak-lined T Tauri stars

G. Duvert[1], **S. Guilloteau**[2], **F. Ménard**[3,1], **M. Simon**[1,4], **and A. Dutrey**[2]

[1] Laboratoire d'Astrophysique de Grenoble, B.P. 53, 38041 Grenoble Cedex 9, France
[2] Institut de Radio Astronomie Millimétrique, 300 Rue de la Piscine, 38406 Saint Martin d'Hères Cedex, France
[3] Canada-France-Hawaii Telescope Corp., P.O.Box 1597, Kamuela, HI 96743, USA
[4] Department of Physics and Astronomy, State University of New York, Stony Brook, NY 11794 3800, USA

Received 8 February 1999 / Accepted 12 November 1999

Abstract. We present the results of a search for dust and gas emission around T Tauri stars in the Taurus-Auriga region, conducted with the IRAM interferometer in CO, HCO^+ and the adjacent continua at 1.3 and 3.4 mm. We studied a sample of young stars with and without the near-infrared spectral signature of disks, to learn whether young stars with little or no evidence of inner accretion disks are surrounded by extensive outer disks providing reservoirs of cold gas and dust.

Our sample comprises 3 classical T Tauris (TTs) and 12 weak-lined T Tauris (WTs). We detect the thermal emission indicative of the presence of a disk around the TTs: IP Tau, LkCa 15 and HP Tau. We resolve the continuum emission of the dust disk of LkCa 15. We also resolve the CO and HCO^+ emission of a large rotating disk at LkCa 15. We do not detect any millimeter continuum or CO emission from the WTs, with the notable exception of V 836 Tau, a borderline WT presenting evidence of accretion activity.

Our detection limits place stringent upper bounds on the amount of circumstellar gas and dust left around the WTs. Our detection of all the TTs and non-detection of all the WTs indicate that the disappearance of disks in TTs, and the corresponding time scale for this disappearance, customarily derived from infrared observations that sample the hot inner part of circumstellar disks ($R \leq 5$ AU), concerns in reality the entire disk, including the outer regions ($R \geq 50 - 500$ AU) to which our observations are more sensitive.

Key words: stars: circumstellar matter – stars: pre-main sequence – stars: rotation – stars: variables: general – radio continuum: stars – radio lines: stars

1. Introduction

Young dwarf stars are not born alone. Often they have at least one companion and appear surrounded by dust. Theories of star formation interpret this dusty environment, radiating in the near-infrared and longer wavelengths, as a flat, rotation-supported, disk of gas and dust orbiting the star (Shu et al. 1987). Millimeter interferometry has enabled some of these disks to be resolved in their continuum and line millimeter emission (e.g. Dutrey et al. 1994, Koerner & Sargent 1995). The high angular resolution possible in the visible and near infrared using the Hubble Space Telescope and adaptive optics techniques from the ground has made it possible to image the inner parts of the disk in the scattered light of the central star (Roddier et al. 1996; Stapelfeldt et al. 1998).

The signature of a star's youth is also found in its optical spectrum. It is customary to distinguish two classes among the low mass young stars, the classical T Tauris, TTs, and the weak emission-line T Tauris, WTs, according to whether their Hα equivalent width is greater or less than 10 Å (e.g. Herbig and Bell 1988, HBC). Within a given star forming region, TTs and WTs appear to share similar masses, ages, luminosity and kinematics (Walter et al. 1988).

If one supposes that the TTs evolve into WTs, the time interval over which the disks disappear must be short, $\leq 10^5$ yr because only a few stars with the near and far-IR spectral signature of "dissipating disks" have been identified (Skrutskie et al. 1990; Simon & Prato 1995; Wolk & Walter 1996). It is not known whether disks disappear by draining of the external reservoir of material or by first clearing the inner regions when dust grains grow in size in the process of planetesimal and planet formation. The optical and near-infrared spectral signatures of a disk around a PMS star sample only the inner few AU of the circumstellar dust disk and do not give any measure of the related gas content. Millimeter wavelength continuum and spectral line observations provide the means to assess the presence of a large reservoir of dust or gas at greater distances from the star.

In a previous paper, we surveyed the dust and gas distribution around a sample of TTs by CO and continuum observations at 2.7 mm (Dutrey et al. 1996). We found the dust disks to be more extended than previously thought, with a lower limit on the typical radius of 150–200 AU, and a relatively flat surface density law ($\Sigma(r) \propto r^{-p}$, with $p < 1.5$), implying that the mass distribution may be dominated by the outer regions. This suggests that the lack of excess emission in the IR among the WTs does not necessarily imply low disk masses. The goal of our observations was to search for the presence of extensive outer disks of gas and dust around young stars without prominent indicators of the classic T Tauri phenomena and thus to seek

Send offprint requests to: G.Duvert (duvert@obs.ujf-grenoble.fr)

Table 1. Properties of the selected sample.

Field	HBC Num.	Name(s)	R.A. (J2000.0)	DEC. (J2000)	Sp.T.	Class.	log Age (yr)
1	352[b]	NTTS035120+3154SW	03 54 29.4	+32 03 01.6	G0(Li?)		>8
1	353[b]	NTTS035120+3154NE	03 54 30.0	+32 03 01.5	G5	WT	>8
2	356,357	NTTS040012+2545N,S	04 03 14.0	+25 52 59	K2	WT	7.6
3	360[b]	NTTS040142+2150SW	04 04 39.2	+21 58 20	M3	WT	6.3
3	361[b]	NTTS040142+2150NE	04 04 39.7	+21 58 22	M3	WT	6.3
4	372	NTTS041529+1652	04 18 21.4	+16 58 46	K5(Li)	WT	8.0
5	378	V819 Tau	04 19 26.30	+28 26 13.5	K7+?	WT	6.0
6	385	IP Tau	04 24 57.02	+27 11 58.2	M0Ve	TT	5.6
7	397	L1551-51	04 32 09.30	+17 57 22.6	K7	WT	7.5
8	407	NTTS043124+1824	04 34 18.01	+18 30 06.6	G8	WT	>8
9		NTTS043220+1815	04 35 14.20	+18 21 35.5	F8	WT	>8
10	66	HP Tau	04 35 52.8	+22 54 23.43	K3	TT	6.2
10	414[t]	HP Tau G3	04 35 53.42	+22 54 09.7	K7+?	WT(bin[1])	$6.0^{+.5}_{-.3}$
10	415[t]	HP Tau G2	04 35 54.07	+22 54 13.8	G0nIII	SU Aur	6.5
11	419	LkCa 15	04 39 17.76	+22 21 03.7	K5IV[2]	TT	6.0
12	429	V 836 Tau	05 03 06.54	+25 23 19.6	K7-M0[2]	WT	5.9

[b] following the catalog number indicates a binary whose companion appears also in this table. [t] similarly indicates a triple system.
References: 1: Simon et al. 1995, 2: Wolk & Walter 1996.

evidence of an evolutionary link between the TTs and WTs. This paper describes our results.

2. Observational procedure

2.1. Dust and molecular lines

We chose to observe in the ^{12}CO (J=2–1) line at 1.3 mm because it provides high sensitivity to the presence of circumstellar gas and high angular resolution (Dutrey et al. 1997). We also observed simultaneously the (J=1–0) rotational line of HCO^+ at 3.4 mm because this line arises in regions of critical density 20 times larger than CO. The HCO^+ molecule, although depleted by a factor of ~ 10 in circumstellar disks (Dutrey et al. 1997), is still the most abundant of the tracers of higher density gas. Simultaneous broad-band observations at 3.4 mm and 1.3 mm probed the continuum emission of the dust.

2.2. Observed sample

We selected the stars observed from the WTs in the Taurus star forming region (SFR) described by Strom et al. (1989) and Wolk & Walter (1996). We adopt 140 pc as the distance to the SFR. We tried to select stars away from known CO emission of the SFR because its presence could complicate the interpretation. With the exception of the HP Tau region, we were successful in this. We also tried to select stars spanning a wide range of ages to explore possible evolutionary effects. Table 1 lists the interferometer field number, HBC catalog number, name, spectral type, classification and age estimate of the stars. These ages (Column 8) are estimates calculated using the procedure described by Simon & Prato (1995). We used K-band magnitudes from the literature. For stars whose ages were also estimated by Hartigan et al. (1995), the agreement is quite good, generally within a factor 3 to 4 (a typical confidence interval is given for the star HP Tau G3). Most stars in the sample are older than 1 Myr. The entire sample consists of 12 WTs and 3 TTs, some of which are binaries (binarity is indicated as a superscript of the HBC number in Table 1). Osterloh and Beckwith (1995) observed all the stars except L1551-51 in the continuum at 1.3 mm. We note that Neuhäuser et al. (1997) consider NTTS 035120+3154 SW to be a main sequence star at < 60 pc distance.

2.3. Interferometer observations

Observations were carried out with the IRAM Plateau de Bure Interferometer between September and November 1997, using 4 antennas operating in the compact ("D") configuration and snapshot mode (4 sources per transit), giving a typical beam size of $\sim 3''$ at 1.3 mm and $\sim 6''$ at 3 mm. We observed simultaneously at 89.2 GHz (HCO^+) and 230.5 GHz (CO) in the lower side-band. The back end was a correlator with one band of 20 MHz centered on the CO (J=2–1) line, one band of 10 MHz centered on the HCO^+ (J=1–0) line, 3 overlapping bands of 160 MHz giving an equivalent bandwidth of 440 MHz for the 1.3 mm continuum and one 140 MHz-wide band for the 3.4 mm continuum. The original spectral resolution was $0.1\,\mathrm{km\cdot s^{-1}}$ and $0.13\,\mathrm{km\cdot s^{-1}}$ in the HCO^+ and CO spectral band, respectively.

The phase and flux calibrators were 0415+379 and MWC349. The rms phase noise was between 10° and 20° at 3.4 mm and between 25° and 40° at 1.3 mm. The position errors produced by the phase noise were smaller than $0.1''$. During our observations, the flux of the calibrator, 0415+379, varied from 2.9 Jy (September) to 3.4 Jy (late October) at 3.4 mm, and from 1.3 Jy to 1.8 Jy at 1.3 mm. The seeing, estimated from the calibrator data, was consistently below $\sim 0\farcs7$. We used the GILDAS software package to reduce the data. The continuum

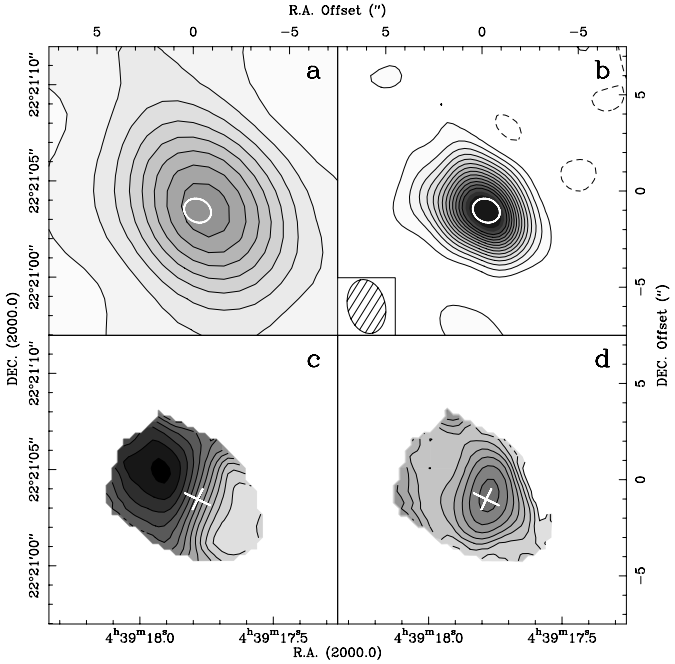

Fig. 1a – d. Images of LkCa 15: **a**: HCO^+ integrated intensity map, contours are 0.25 to $2.0\,\mathrm{K\cdot km\cdot s^{-1}}$ by steps of $0.25\,\mathrm{K\cdot km\cdot s^{-1}}$. An ellipse marks the position and size of the uv plane fitting of the 1.3 mm continuum. **b**: CO J=2-1 integrated intensity map, contours are -1 to $15\,\mathrm{K\cdot km\cdot s^{-1}}$ by steps of $1\,\mathrm{K\cdot km\cdot s^{-1}}$. Continuum emission is indicated as in panel (**a**). **c**: isovelocity contours of the CO emission, contours are 5.35 to $7.0\,\mathrm{km\cdot s^{-1}}$ by $0.25\,\mathrm{km\cdot s^{-1}}$. The figure is limited to the inside of the $0.5\,\mathrm{K\cdot km\cdot s^{-1}}$ contour of panel (**b**). The cross plots the main axes of the ellipse fitted to the 1.3 mm continuum emission. **d**: linewidth of the CO emission, contours are 1.5 to $3.25\,\mathrm{km\cdot s^{-1}}$ by $0.25\,\mathrm{km\cdot s^{-1}}$. Cross as in (**c**).

images are the results of summing the lower and the upper sideband data. We used natural weighting of the visibilities during all the image processing.

3. Results

We observed 12 interferometer fields. The average integration time of 4 hours per field produced typical rms noise of 0.9 mJy in the 1.3 mm continuum and 0.8 mJy at 3.4 mm. Since the primary beam of the interferometer is $\approx 22''$ (FWHP) at 1.3 mm, each pointing always included the companions of the multiples and in some cases more than one of the targets. We detected continuum emission at 1.3 mm and 3.4 mm from LkCa 15, V 836 Tau, HP Tau (detected in the continuum at 3.4 mm at the edge of the HP Tau G2 field), and IP Tau (see Table 2). The 3σ detection limit in the continuum at 1.3 mm was ≈ 2.5 mJy.

We detected the CO line at LkCa 15, V 836 Tau, and HP Tau G2, and HCO^+ at LkCa 15. For the non-detections, assuming a total line width of 4 $\mathrm{km\cdot s^{-1}}$ the typical upper limit on CO line flux is 0.5 Jy. $\mathrm{km\cdot s^{-1}}$ at the 3 σ level. The following subsections discuss the sources in which we detected the mm-wave continuum and CO line.

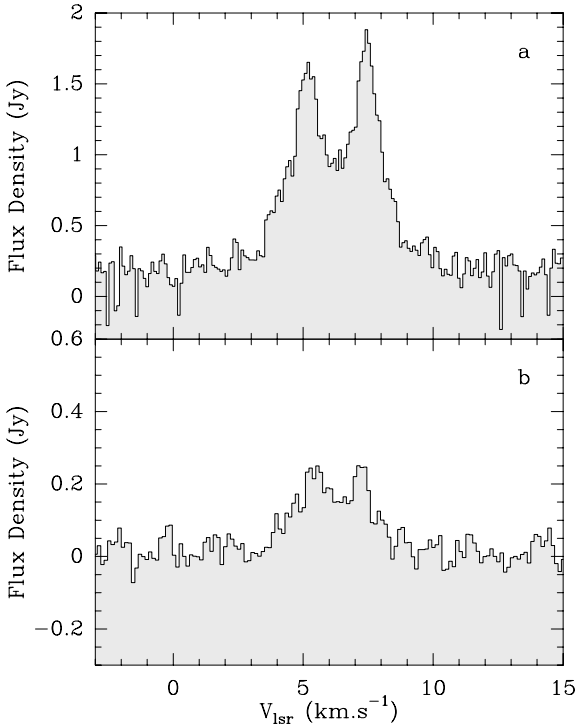

Fig. 2. Spectra of LkCa 15: **a**: CO (J=2-1) spectrum. **b:** HCO^+ (J=1-0) spectrum.

Table 2. Continuum detections

Name	S_ν(3.4 mm) (mJy)	S_ν(1.3 mm) (mJy)	S_ν(1.2 mm) (mJy)
LkCa 15	10 ± 0.8	124 ± 3	167 ± 6[a]
V 836 Tau	3.0 ± 0.8	24 ± 2	37 ± 6[a]
	7.7 ± 1.2[b,†]		
HP Tau	9.4 ± 1.0		62 ± 6[c]
IP Tau	1.7 ± 0.7	9 ± 1	16 ± 5[a]

References: [a]: Osterloh & Beckwith 1995, [b]: Paper 1, [c]: Beckwith et al. 1990

[†]: Flux measured at 2.7 mm.

3.1. LkCa 15

The HBC classifies LkCa 15 as a WT but Wolk & Walter (1996) measured $W_\lambda(H_\alpha)= 21.9$Å. We follow Bouvier et al.'s (1995) reclassification of it as a TT.

The spectral index of the continuum emission we detected is $\alpha = 2.6 \pm 0.1$ (in the sense $S_\nu \propto \nu^\alpha$) which indicates it arises in the thermal emission of dust. The 1.3 mm continuum emission is resolved: fitting a two-dimensional Gaussian in the uv plane gives a value of $(1\farcs45 \pm 0.08) \times (1\farcs2 \pm 0.08)$ at PA=$64° \pm 13°$. Assuming the elongation is attributable to the projection of an inclined thin circular disk, its inclination is $34° \pm 10°$. Figs. 1 and 2 summarizes our spectral line observations of LkCa 15. The velocity gradient of the CO emission lies along the major axis of the integrated emission (Fig. 1c), which is coincident with that of the continuum emission. This is the unambiguous signature of rotation (e.g., Koerner & Sargent 1995, Guilloteau

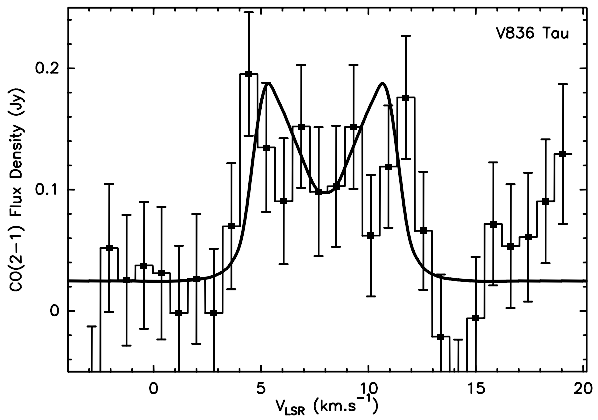

Fig. 3. Spectrum of CO (J=2-1) detected towards V 836 Tau. The original spectrum was smoothed to $0.8\,\mathrm{km\cdot s^{-1}}$ velocity resolution to improve signal to noise ratio. Errorbars are plotted for each channel. The thick line is the expected profile for the disk model described in the text.

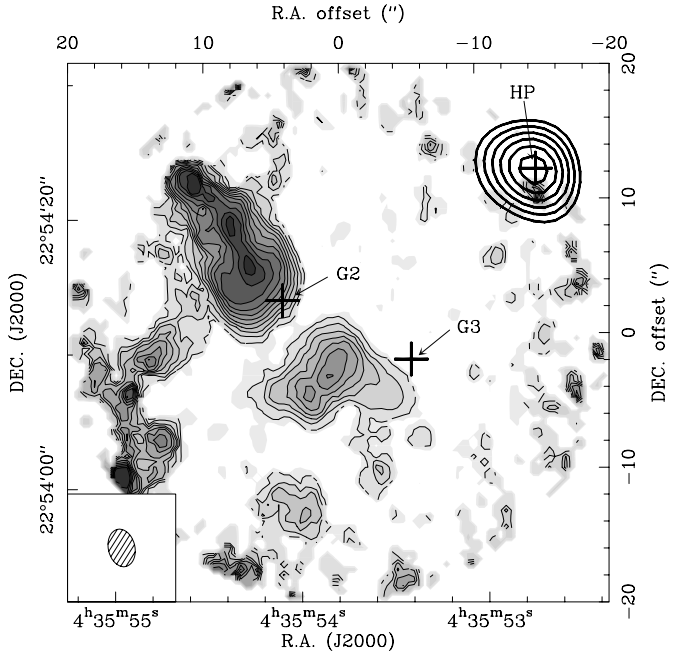

Fig. 4. The HP Tau region. Crosses indicate the position of HP Tau G2, G3 and HP Tau. Shaded contours show the CO (J=2-1) integrated area showing the bipolar emission around HP Tau G2. Contours are 0.1 to $1.1\,\mathrm{K\,km\,s^{-1}}$ in $0.1\,\mathrm{K\,km\,s^{-1}}$ increment. The heavy unshaded contours trace the 3.4 mm continuum peak detected (levels 4 to 9 mJy by 1 mJy) towards HP Tau.

& Dutrey 1998). The CO and HCO^+ observations show that the rotating disk is large with outer radius ~ 600 AU, and the channel maps show that the intrinsic linewidth must be small ($< 0.3\,\mathrm{km\cdot s^{-1}}$) as also found for the rotating disks of GM Aur and DM Tau (Dutrey et al. 1998, Guilloteau & Dutrey 1998). Aperture synthesis mapping with better uv-plane coverage of LkCa 15 has since been obtained with the IRAM interferometer and a more thorough analysis will be published in a forthcoming paper.

3.2. V 836 Tau

The 9Å Hα equivalent width and near infrared colors of V 836 Tau mark it as an object with properties intermediate between that of the WTs and TTs (HBC; Skrutskie et al. 1990; Hartigan et al. 1995; Prato and Simon 1997). Our detection of V 836 Tau in the continuum at 1.3 mm is consistent with Skinner et al.'s (1991) and Osterloh and Beckwith's (1995) earlier measurements. The spectral index of the continuum radiation, using all the available data between 0.8 mm and 3.4 mm (Skinner et al. 1991; Beckwith et al. 1990) is $\alpha = 2.2 \pm 0.2$. Clearly the continuum emission is thermal but whether it is actually optically thick, as the simplest interpretation of the spectral index indicates, or optically thin radiation of dust with an unusual wavelength dependence of its dust opacity, essentially flat, or dust opacity with a normal wavelength dependence (e.g. Beckwith et al. 1990) but residing in a highly inclined disk cannot be determined from the present data. Measurements over a larger wavelength range and observations that resolve the emission could distinguish between the possibilities.

The CO emission of V 836 Tau is detectable (Fig. 3), but so weak that we could not map it. The integrated line flux is $0.84 \pm 0.18\,\mathrm{Jy\,km\cdot s^{-1}}$. The line has a remarkably large width $7.0 \pm 1.4\,\mathrm{km\cdot s^{-1}}$, centered at V_{LSR} = $7.6 \pm 0.8\,\mathrm{km\cdot s^{-1}}$. The linewidth suggests an origin in a rotating disk observed at large inclination. The spectrum is compatible with that expected from a disk ~ 120 AU in radius, in Keplerian rotation around a $\sim 1\,\mathrm{M_\odot}$ star, and seen nearly edge on. The fact that we do not resolve the disk's continuum emission in our $\sim 3''$ beam is consistent with this interpretation. As an illustration, we have plotted the CO line profile expected for such a disk (inclined by $\simeq 80°$ along the line of sight) over the observed spectrum in Fig. 3.

3.3. The HP Tau region

Our observation included HP Tau G2,HP Tau G3, and HP Tau in one interferometer pointing. HP Tau G2 is a SU Aur-type star that forms a hierarchical triple with HP Tau G3, 9.9″ away. HP Tau G3 itself is a close double (Richichi et al. 1994). The triple and HP Tau (at $21''$ distance and P.A. $298°$), are surrounded by a large arclike reflection nebula $30''$ in radius.

Fig. 4 summarizes our observations of this region. Continuum radiation was detected only from HP Tau. Table 2 lists the flux measured at 3.4 mm. Our observations also detected HP Tau at 1.3 mm. We prefer not to report a 1.3 mm flux because HP Tau lay well outside the primary beam of the interferometer at that frequency, so the correction for the primary beam response is large and uncertain. The spectral index between our measurement at 3.4 mm and Osterloh & Beckwith's (1995) measurement at 1.3 mm is 2.0 ± 0.1 indicating thermal emission.

Our observations detected strong and extended CO emission in the vicinity of HP Tau G2 and weak CO emission is present throughout the map. This was to be expected since the existence of a reflection nebula hints at the presence of a background molecular cloud. The CO emission near HP Tau G2 con-

sists of two lobes $5''$ wide on either side of HP Tau G2, oriented in an approximately NE-SW direction. Fig. 4 shows this emission in grey-filled contours. To show the CO emission extent in Fig. 4 the map has been corrected for primary beam attenuation, thus severely increasing the noise level in its outer parts. The NE lobe is truncated by the main beam of the interferometer and may extend farther away from the star than the map suggests. (Besides the effects of attenuation by the primary beam response, we note that our interferometric observations are not sensitive to large-scale structure.) The emission is elongated (with a minimum of 3:1 ratio) and aligned exactly with HP Tau G2. The velocity gradient in the faint SW CO lobe is marginal ($V_{LSR} = 10.5 \pm 0.2\,km\cdot s^{-1}$), but there is a clear trend in the NE lobe to reach greater (red-shifted) velocities farther from G2, with velocities of $\sim 8.2\,km\cdot s^{-1}$ near the star to $\sim 10.2\,km\cdot s^{-1}$ at the NE end of the CO lobe. This structure, clearly associated with HP Tau G2, with a maximum of emission at the position of the background molecular cloud, can be interpreted as a lobe of a bipolar outflow from the HP Tau G2 star.

3.4. IP Tau

IP Tau is a relatively weak source of continuum emission (Table 2). The spectral index between 3.4 and 1.3 mm is 1.7 ± 0.6 consistent with that expected for thermal dust emission. No CO emission was detected at an upper limit of 0.5 Jy $km\cdot s^{-1}$ (3σ).

4. Discussion

We have detected continuum emission consistent with the thermal radiation of dust from all the TTs in our sample, LkCa 15, HP Tau, and IP Tau, and also from V 836 Tau, a WT whose observed properties are regarded as intermediate between the TTs and WTs. We detected circumstellar CO line emission only from LkCa15 and V 836 Tau; the CO emission of HP Tau G2 seems to arise in a bipolar outflow. Our observations resolve both the continuum and CO emission of LkCa 15 and indicate an origin in a rotating disk. The continuum and line emission of V 836 Tau are consistent with an origin in a rotating disk of radius ~ 120 AU.

As regards the non-detections, the 2.5 mJy upper bound in the continuum at 1.3 mm (Sect. 3) corresponds to an upper bound of $\approx 2 \times 10^{-4}\,M_\odot$ if this emission arises in an optically thin dust disk with emissivity as given in Dutrey et al. (1996), mean disk temperature of 30 K, and gas-to-dust ratio of 100. Alternatively, it implies disk sizes smaller than about 4 AU if the emission is optically thick. The mass upper bound set by the upper limit on the CO (J=2–1) line emission is even more stringent. If the CO emission is optically thin, and using standard abundances (Frerking et al. 1982), the upper limit corresponds to an upper limit of $\sim 6 \times 10^{-7}\,M_\odot$ for the mass. If CO is depleted with respect to H_2, the upper bound for the mass would be correspondingly higher.

Although binaries with separations smaller than ~ 100 AU are weaker mm-wave continuum sources than the single stars or wide binaries, apparently the result of gaps in the disks produced by tidal interactions (Osterloh & Beckwith 1995; Jensen et al. 1996), it seems unlikely that multiplicity affects the rate at which we detected the WTs. With the exception of HP Tau G3 (separation $\sim 1''$) and NTTS040012+2545 (separation $0.021''$, all the binaries in our sample are wide, at separation $\approx 10''$, corresponding to ~ 1400 AU at the distance of the SFR. The actual physical separations are larger because the angular separations are projected values. Separations > 1400 AU would be sufficient to accommodate disks around at least one of the stars if their sizes were similar to those around single stars, for example ~ 525 AU for GM Aur (Dutrey et al. 1998) or 800 AU for DM Tau (Guilloteau & Dutrey 1998).

In any case, our detection rate for extensive gaseous disks associated with the WTs is 1 (V 836 Tau) out of 12 systems. This figure does not change if we consider now the *continuum detections of WTs* and is indistinguishable from Osterloh & Beckwith's (1995) detection rate of 1.3 mm emission from the WTs, 11%, and Wolk & Walter's (1996) detection rate of IR emission among X-ray selected young stars, the naked T Tauri stars (2 out of 39). It is also comparable to the rate of detection of WTs in Dutrey et al. (1996) sample: only one WT was detected on a total of 9, and this WT was V 836 Tau. Our rate of detection in the continuum for the TTs (100%) is markedly different, and comparable (owing to the small sample size) to the rate of detection (18 out of 24) of dust disks around TTs at 2.7 mm by Dutrey et al. (1996).

We point out that different observational techniques sample quite distinct regions of the circumstellar environment of T Tauri stars. UV excess and optical veiling arise in the innermost accretion region ($R \leq 0.1$ AU), and the IR excess typically originates from $R \leq 5$ AU from the star (the *"IR disk"*). Although the mass distribution may be dominated by the outer part of the disk (Dutrey et al. 1996), the continuum, being mostly optically thin, traces the product of the radial kinetic temperature by the surface density distribution, $T(r) \times \Sigma(r)$, and the bulk of the mm continuum emission comes from $10 \leq R \leq 100$ AU (the *"mm disk"*). In contrast, due to its much higher optical depth, CO emission traces $T(r)$, and, because of beam dilution, observations are only sensitive to the outer disk parts ($50-100 \leq R \leq 1000$ AU, the *"CO disk"*, e.g. Dutrey et al. 1998, Duvert et al. 1998).

The observations presented in this paper are not sensitive to the properties of the IR disk from which originate *all* the visible and infrared emission used in the literature to classify and discuss the properties of WTs and TTs, but only to the characteristics of the mm and CO disks. We detect both mm and CO disks in TTs, we detect none of them in WTs. Furthermore, in the only borderline case of our sample, V 836 Tau, we detect only weak mm emission, and a very small CO disk.

It thus appears that the markedly different spectral signatures of WTs and TTs in the visible and near-infrared (Skrutskie et al. 1990; Hartigan et al. 1995) are reflected in our observations that probe outer, colder regions of circumstellar disks. This parallel behavior strengthens one hypothesis that motivated this work, that the millimeter continuum, molecular emission and excess

IR emission share a common physical origin in a circumstellar disk.

The idea that TTs evolve to WTs is common in the literature (Lada 1987, Lada 1999 and references therein). Several authors have used statistical arguments, based on the detection rate of the near and mid-IR spectral signature of "dissipating disks", to estimate the time scale of disk disappearance. They obtain a time scale less than 10^5 yr and even $\leq 2 \times 10^4$ yr in some cases (Skrutskie etal 1990, Simon & Prato 1995, Wolk & Walter 1996). Our small sample of objects is not suited to derive independently an estimate for this time scale. However, under the assumption that TTs evolve in WTs, it shows that the entire disks, and not only the IR disk, disappear on these time scales.

5. Conclusions

The observational technique used here sample regions of circumstellar disks that are distinct and complementary to IR and shorter wavelength observations. We detected millimeter continuum and CO emission in all the TTs, and none in the WTs, with the exception of the borderline case V 836 Tau that has a weak mm emission and very small CO disk. That the dichotomy between TTs and WTs is still present in our spectral domain of observation indicates that the disappearance of disks in TTs – and the corresponding time scale for this disappearance – derived from IR observations of inner regions of circumstellar disks ($R \leq 5$ AU), apply to the entire disk, including the outer regions ($R \geq 50 - 500$ AU) sampled by our observations.

Acknowledgements. G.D. warmly thanks S.Cabrit and J. Bouvier for their comments at an early stage of this paper. We used SIMBAD which is operated at CDS, Strasbourg, France. The work of M. Simon was supported in part by NSF Grant AST 94-17191.

This paper is dedicated to the memory of the victims of the tragic accident of the Plateau de Bure cable car, where five of our IRAM colleagues and fifteen employees of other companies lost their lives while working to advance scientific research.

In Memoriam

Bernard AUBEUF	*Sylvain AUBRY*
Michel CANNONE	*Romain DELFOSSE*
Mickael EYMEOUD	*Francis GILLET*
Henri GONTARD	*Lucien KOUBI*
François MACE	*Pascal MAHE*
Norbert MERELLA	*Bruno NOUGIER*
Stéphane PARIS	*Roland PRAYER*
Michel ROUGNY	*Jean SABAR*
Fabien TONDA	*Senol TOPAL*
Patrick VIBERT	*Frédéric VILLAR*

References

Beckwith S.V.W., Sargent A.I., Chini R.S., Güsten R., 1990, AJ 99, 924
Bouvier J., Covino E., Kovo O., et al., 1995, A&A 299, 89 1997, AJ, 113, 740
Dutrey A., Guilloteau S., Simon M., 1994, A&A 286, 149
Dutrey A., Guilloteau S., Duvert G., et al., 1996, A&A 309, 493
Dutrey A., Guilloteau S., Guélin M., 1997, A&A 317, L55
Dutrey A., Guilloteau S., Prato L., et al., 1998, A&A 338, L63
Duvert G., Dutrey A., Guilloteau S., et al., 1998, A&A 332, 867
Frerking M.A., Langer W.D., Wilson W.L., 1982, ApJ 262, 590
Guilloteau S., Dutrey A., 1998, A&A 339, 467
Hartigan P., Edwards S., Ghandour L., 1995, AJ 452, 536
Herbig G.H., Bell K.R., 1988, Third Catalog of Emission-line Stars of the Orion Population. Lick Obs. Publ, 1111, 1988 (HBC)
Jensen E.L.N., Mathieu R.D., Fuller G.A., 1996, ApJ 458, 312
Koerner D.W., Sargent A.I., 1995, AJ 109, 2138
Lada C.J., 1987, In: Peimbert M., Jugaku K. (eds.) Star Forming Regions. IAU Symposium 115, Reidel, Dordrecht, p. 1
Lada C.J., 1999, In: Lada C.J., Kylafis N.D. (eds.) The Origin of Stars and Planetary Systems. Kluwer, Dordrecht, p. 143
Neuhäuser R., Torres G., Sterzik M.F., Randich S., 1997, A&A 325, 647
Osterloh M., Beckwith S.V.W., 1995, ApJ 439, 288
Prato L., Simon M., 1997, ApJ 474, 455
Richichi A., Leinert Ch., Jameson R., Zinnecker H., 1994, A&A 287, 145
Roddier C., Roddier F., Northcott M.J., Graves J.E., Jim K., 1996, ApJ 463, 326
Shu F.H., Adams F.C., Lizano S., 1987, ARA&A 25, 23
Simon M., Ghez A.M., Leinert Ch., et al., 1995, ApJ 443, 625
Simon M., Prato L., 1995, ApJ 450, 824
Skinner S.L., Brown A., Walter F.M., 1991, AJ 102, 1742
Skrutskie M.F., Dutkevitch D., Strom S.E., et al., 1990, AJ 99, 1187
Stapelfeldt K.R., Krist J.E., Ménard F., et al., 1998, ApJ 502, L65
Strom K.M., Strom S.E., Edwards S., Cabrit S., Skrutskie M.F., 1989, AJ 97, 1451
Walter F.M., Brown A., Mathieu R.D., Myers P.C., Vrba F.J., 1988, AJ 96, 297
Wolk S.J., Walter F.M., 1996, AJ 111, 2066